ISSN 0031-918X, Physics of Metals and Metallography, 2017, Vol. 118, No. 3, pp. 279–287. © Pleiades Publishing, Ltd., 2017.
Original Russian Text © I.Yu. Khmelevskaya, R.D. Karelin, S.D. Prokoshkin, V.A. Andreev, V.S. Yusupov, M.M. Perkas, V.V. Prosvirnin, A.E. Shelest, V.S. Komarov, 2017, published in Fizika Metallov i Metallovedenie, 2017, Vol. 118, No. 3, pp. 293–300.

STRUCTURE, PHASE TRANSFORMATIONS, AND DIFFUSION

Effect of the Quasi-Continuous Equal-Channel Angular Pressing on the Structure and Functional Properties of Ti–Ni-Based Shape-Memory Alloys

I. Yu. Khmelevskaya[a, *], R. D. Karelin[a, c], S. D. Prokoshkin[a], V. A. Andreev[b], V. S. Yusupov[c], M. M. Perkas[c], V. V. Prosvirnin[c], A. E. Shelest[c], and V. S. Komarov[a]

[a] *National University of Science and Technology MISiS, Leninskii pr. 4, Moscow, 119049 Russia*
[b] *Matek-Sma Ltd, ul. Kar'er 2a, Moscow, 117449 Russia*
[c] *Baikov Institute of Metallurgy and Materials Science, Russian Academy of Sciences, Leninskii pr. 49, Moscow, 119991 Russia*
**e-mail: khmel@tmo.misis.ru*

Received August 18, 2016; in final form, September 30, 2016

Abstract—The effect of severe plastic deformation by equal-channel angular pressing (ECAP) under normal and quasi-continuous regimes on the structure and the mechanical and functional properties of a Ti–50.2 at % Ni shape-memory alloy (SMA) has been studied. ECAP was carried out at an angle of intersection of channels of 120° in the normal regime with heating between passes at 450°C for 20 passes and in the quasi-continuous regime at the temperature of 400°C for three, five, and seven passes. The hot screw rolling with subsequent annealing at 750°C for 30 min and cooling in water was used as a control treatment (CT). A mixed submicrocrystalline and nanosubgrained structure was formed. The increase in the number of passes from three to seven led to a decrease in the average size of structural elements from 115 ± 5 to 103 ± 5 nm and to an increase in the fraction of grains/subgrains having a size less than 100 nm. After ECAP (seven passes) and post-deformation annealing at the temperature of 400°C for 1 h, a completely recoverable strain was 9.5%; after normal ECAP, 7.2%; after CT, 4.0%.

Keywords: shape-memory alloys, titanium nickelide, thermomechanical treatment, nanostructure, equal-channel angular pressing, functional properties

DOI: 10.1134/S0031918X17030073

INTRODUCTION

Nowadays, the method of severe plastic deformation (SPD) by equal-channel angular pressing (ECAP) and some its modifications are the most promising processes to produce bulk billets of shape-memory alloys (SMA) with an ultrafine-grained (UFG) structure [1–24]. ECAP in parallel channels, multichannel ECAP, and ECAP–Conform make it possible to increase the degree of deformation by several times in order to substantially decrease the total number of passes for the formation of the UFG structure, as well as to increase the utilization coefficient of the material to values close to 0.95.

In [7, 15, 21, 22], it was shown on Ti–Ni-based SMAs that the ECAP with an angle of intersection of channels of 110° and six to eight passes at the temperature, which does not exceed 450°C, provides the formation of mainly an equiaxed ultrafine-grained submicrocrystalline structure of the *B*2 austenite. For the further refinement of the grain, the number of passes was increased, and the deformation temperature was decreased. However, even after ECAP at 350°C, the grain size remained in the submicrometer range of sizes (100–1000 nm) [15], whereas it is a nanocrystalline structure with the grain size of 40–80 nm, which is the most effective in terms of functional properties [16]. The reason that prevents the refinement of the austenite grain upon traditional ECAP is the use of intermediate heatings to the deformation temperature between passes [20]. A possibility of producing the nanocrystalline structure can be associated with the change in the basic parameters of the ECAP process. The increase in the angle of intersection of channels to 120° makes it possible to decrease the resistance to deformation upon the decrease in the deformation temperature. The exclusion of interpass heatings should prevent the growth of structural elements. Therefore, it is desirable to carry out the ECAP process continuously under isothermal conditions.

In this context, the timekeeping of the ECAP process with the intersection angle of channels equal to 120° (more than in [15]) at a temperature of 400°C was performed. The heating of the billet after each pass was

Table 1. Treatment regimes

No.	Treatment regimes				
	ECAP			Annealing	
	temperature, °C	number of passes	angle of intersection of channels, deg	temperature, °C	heating, min
1	450	20	120	–	–
2	400	3	120	–	–
3	400	3	120	400	60
4	400	5	120	–	–
5	400	5	120	400	60
6	400	7	120	–	–
7	400	7	120	400	60

only carried out in the deformation container. The temperature of the billet at the inlet and outlet from the container, the deformation time, and the transfer time of the billet from the outlet channel into the container were fixed. The billet usually had no time to heat up to the temperature of the container in the time including the placement into the container and the deformation time (about 2 min), but was heated due to the effect of shear deformation. The measurements of the temperature of the billet surface before placing into the container and immediately after outlet from the container using a pyrometer give clearly underestimated values (270–300°C). However, the results of the experiment show that in the first two passes out of five passes, the temperature of the billet is lower than in the last passes by only about 30 K apparently due to the heating of the billet during deformation. The value of the increment of the temperature of the sample during ECAP is mainly determined by the strength of the deformed material and by the rate of deformation [25]. In [26], the dependence of the heating of the samples on the deformation rate and on the sample size is reported and the estimation of the heating of samples of three near-equiatomic alloys Ti–Ni during ECAP at room temperature was carried out. According to the calculations, at a very low deformation rate (0.05 s^{-1}), the temperature of the sample increased during ECAP by 34 K [26]. Thus, it can be expected that, due to deformation-induced heating, the sample temperature should be only slightly lower than the container temperature. This can provide the opportunity of using the quasi-continuous and quasi-isothermal deformation upon the ECAP of Ti–Ni SMAs to form in them the nanocrystalline structure. The purpose of this paper was to verify this assumption.

EXPERIMENTAL

The Ti–50.2 at % Ni alloy to be studied was melted at the Matek-SMAa Ltd. The billet for the ECAP was a rod 20 mm in diameter produced by the method of hot screw rolling (SR) using several passes with a reduction of 7–20% per pass and interpass heatings at 850–950°C (hot-rolled state). As a control treatment (CT) of the samples before ECAP, the annealing at a temperature of 750°C for 30 min with subsequent cooling in water was used. Billets with lengths of 70–100 mm were deformed using an installation in the IMMS RAS with the intersection angle of channels of 120° at temperatures of 450 and 400°C for 3–20 passes.

The ECAP was carried out according to two schemes as follows: (1) deformation for 20 passes at 450°C (ECAP-20) with long breaks between the passes (from several hours to several days) and heating of the billets in a furnace to the deformation temperature and (2) the ECAP was carried out for three to seven passes at 400°C without additional interpass heatings, i.e., quasi-continuously (ECAP-3, ECAP-5, ECAP-7). The regimes of the treatment of the billets are presented in Table 1.

The measurements of the Vickers hardness were carried out at room temperature using a LECOM 400-A tester under a load of 1 N. The structure was studied using X-ray diffraction analysis (a D8 Advance diffractometer) in CuK_α radiation at room temperature and the electron-microscopic method (a JEM-2100 microscope). The mechanical tensile tests were carried out using a Zwick Roell universal device at room temperature at a rate of deformation of 4 mm/min. The recoverable strain was determined using the thermomechanical method upon deformation by bending using template arcs and the method described in [27].

RESULTS AND DISCUSSION

X-Ray Diffractometry

The change in the phase composition of the alloy as a result of ECAP under different regimes was studied using X-ray diffraction analysis (Fig. 1). At room temperature, after a CT, the main phase is *B*19' martensite; the rhombohedral *R*-phase and *B*2 austenite in the amount of no more than 20% are also present. The ECAP-20 leads to a sharp decrease in the amount of the *B*19' martensite and an increase in the amount of the *R* phase compared to the CT. This is caused by an increase in the defectiveness of the lattice with an increasing number of passes and, as a consequence of this, by the stimulation of the $B2 \rightarrow R$ transformation by the fields of stresses of the dislocation substructure [28] and by a decrease in the temperature range of the $R \rightarrow B19'$ forward martensitic transformation, and possibly as a result of the long stay of the alloy in the range of temperatures of the intensive deformation aging (450°C) [28, 29]. After short-term treatments upon ECAP-3, ECAP-5, and ECAP-7, this effect has not yet manifested. The profiles of X-ray diffraction patterns after ECAP 3, 5, and 7 do not differ much from the profile in the state after CT. After ECAP 5, the amount of the *R* phase is greater than after other regimes of ECAP, which can be associated with some inhomogeneity of the chemical composition of the alloy.

The integral estimate of the defectiveness of the crystal lattice can be obtained from the width of the X-ray diffraction line. In our case, this estimate can be only approximate, since the individual lines of *B*2 austenite are not visualized, the (330)–($3\bar{3}0$) doublet of the *R* phase is insufficiently resolved, and most lines of the *B*19' martensite overlap strongly. However, the overlap of the lines indicates their significant broadening caused by the inheritance of martensite-lattice defects (dislocations) from *B*2 austenite, since after the usual quenching from 700–800°C, all lines of the monoclinic *B*19' martensite are clearly separated visually [30]. The width of the (002) line of this quenched *B*19' martensite is $B_{002} = 0.32 \pm 0.03$ deg 2θ [30]; the estimate of the width of this line after ECAP under different regimes yields a significantly greater value (Table 2). Moreover, B_{002} increases with an increasing number of passes upon ECAP, which indicates an increase in the concentration of lattice defects. Annealing at 400°C for 1 h after ECAP-5 and ECAP-7 did not lead to a significant decrease in B_{002}.

Transmission Electron Microscopy

The electron-microscopic study of the structure of the alloy under all regimes of ECAP reveals a very complex structure formed as a result of cooling to room temperature (Fig. 2). The analysis of bright-field and dark-field images and of electron-diffraction patterns shows that there are three main phases, i.e.,

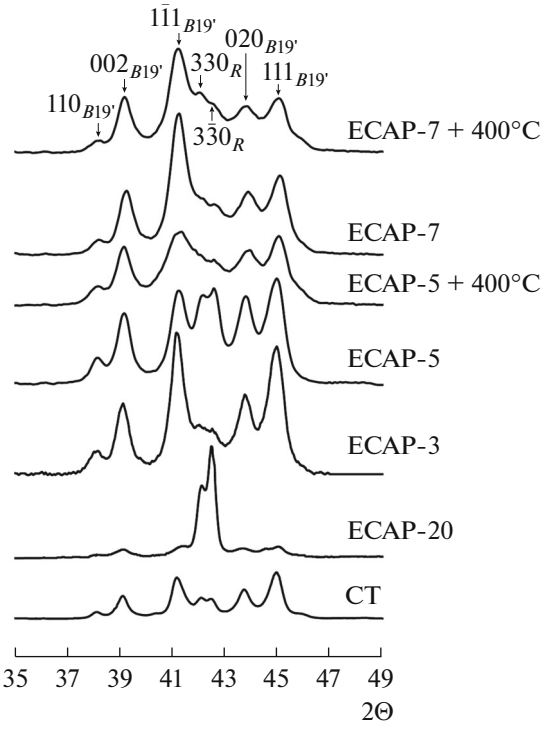

Fig. 1. X-ray diffraction patterns of the Ti–50.2% Ni alloy at room temperature.

*B*19' martensite, *R* martensite, and *B*2 austenite, against the background of a developed dislocation substructure with the density of free dislocations to about 10^{11} cm^{-2} and incompletely equiaxed grains and subgrains of submicron size. In the dark-field images taken in the strong reflections of the first diffraction ring, closely oriented adjacent to each other structural elements (subgrains) and individual bright elements (grains with high-angle misorientations) are observed (Fig. 2).

In the electron-diffraction patterns obtained after different regimes of deformation, both discrete and continuous arc reflections can be observed. The value

Table 2. Width of the (002) X-ray diffraction line of the *B*19' martensite after different treatments

Treatment	B_{002}, deg 2θ (ECAP/ECAP + 400°C, 1 h)
1	0.32 ± 0.03
4	0.44 ± 0.04
5	0.50 ± 0.05
2	0.53 ± 0.05/0.50 ± 0.05
3	0.55 ± 0.05/0.52 ± 0.05

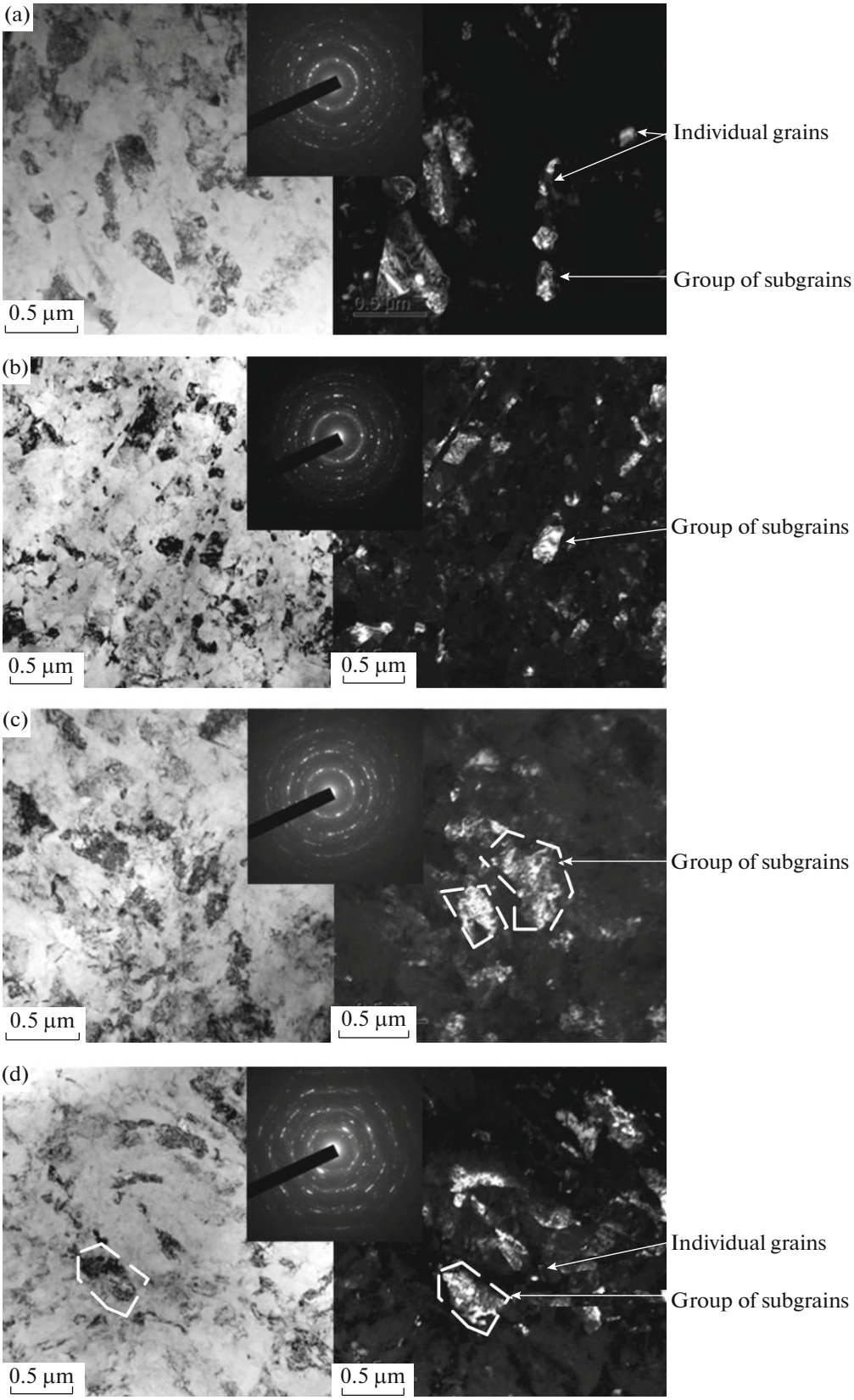

Fig. 2. Microstructure of the Ti–50.2% Ni alloy subjected to deformation according to various regimes: (a) ECAP-20, (b) ECAP-3, (c) ECAP-7, and (d) ECAP-7 + 400°C. Transmission electron microscopy: bright-field images on the left, dark-field images on the right, electron-diffraction patterns in the insets. Examples of individual grains and groups of subgrains are marked by arrows.

of the azimuthal smearing of reflections shows that the misorientation of the crystal lattice in these regions reaches several degrees. Individual point reflections are also present. These electron-diffraction patterns are characteristic of regions with a mixed polygonized (nanosubgrained) and nanocrystalline structure [30, 31].

The statistical analysis of structural elements to determine their average size was carried out using bright-field images in which the boundaries of grains and subgrains are clearly visualized in contrast to the dark-field images, where not all subgrain boundaries are distinguishable. The size of the structural elements was determined without a distinction between boundaries and subboundaries. According to the results of the analysis, in the case of ECAP-20 at 450°C, a mixed ultrafine grain-subgrain structure with sizes of the structural elements (grains and subgrains) of 50–300 nm is formed, as well as a high density of free dislocations. The average linear size of the structural elements was 171 ± 10 nm (Fig. 2); therefore, this structure can be attributed to submicrocrystalline.

The decrease in the deformation temperature to 400°C and the exclusion of interpass heatings lead to a refinement of structural elements. After ECAP-3, a mixed grain-subgrain structure with a large number of grains/subgrains with a size of less than 100 nm was produced. The average linear size of structural elements was 115 ± 5 nm, i.e., it approached the nanometer range from above. With an increase in the number of quasi-continuous passes to seven, the average size of structural elements did not significantly change, rather it stayed at the boundary of the nanometer and submicron ranges (103 ± 5 nm). The high density of free dislocations within the structural elements is retained. Annealing after ECAP-7 at the deformation temperature (400°C, 1 h) visually leads to a decrease in the density of dislocations inside the grains/subgrains (Fig. 2d).

Thus, in the Ti–50.2% Ni alloy subjected to ECAP-7, a mixed nanostructure of *B*2 austenire was produced. The size of structural elements of this nanostructure significantly exceeds the size (40–80 nm, according to [16]) that is optimum from the viewpoint of static functional properties of Ti–Ni SMAs. On the other hand, the mixed nanostructure (grain-subgrain) is more advantageous in terms of fatigue functional properties [32].

Mechanical and Functional Properties

The estimation of the mechanical strengthening achieved as a result of ECAP was carried out using hardness measurements and mechanical tensile tests. The comparison of the results of measurements of the hardness of the Ti–50.2% Ni alloy after all types of the treatment showed a 2.5-fold increase in the hardness after ECAP-7 as compared to the control treatment.

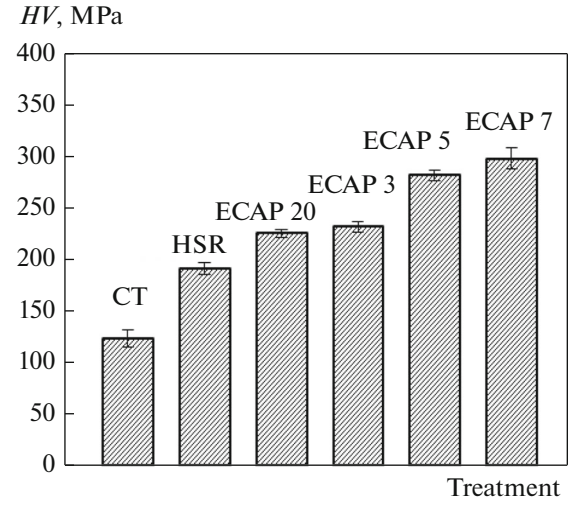

Fig. 3. Dependence of the hardness of the Ti–50.2% Ni alloy on the regimes of TMT.

The hardness after ECAP-20 was comparable to the hardness after quasi-continuous ECAP-3, which indicates partial softening as a result of heating and pauses during ECAP-20 (Fig. 3).

The mechanical behavior of the alloy upon tensile deformation is typical of near-equiatomic Ti–Ni alloys with the structure of martensite. Figure 4 shows the tensile stress–strain diagrams for samples of the Ti–50.2% Ni (at %) alloy after ECAP-3, -5, and -7; in the inset, the following strain and stress parameters are marked: the critical stress of the reorientation of martensite σ_{cr}; dislocation yield stress σ_y; ultimate tensile strength σ_u; and the strain at the yield plateau ε_{pl}, which is an approximate (understated [33]) estimate of the recoverable strain ε_r. The results of the determination of the strain–stress parameters after quasi-continuous ECAP and hot SR are presented in Table 3.

Compared to the hot-rolled state (σ_y = 430 MPa, σ_u = 700 MPa), the alloy after quasi-continuous ECAP-3 and ECAP-7 has higher strength characteristics (σ_u = 1024–1154 MPa). The indicator of plasticity (relative elongation) decreases slightly (to 20% on average). The highest value of the quantity $\Delta\sigma = \sigma_y - \sigma_{cr}$, which is responsible for the realization of the reserve of the recoverable strain [32], was 820–850 MPa after ECAP-5 and ECAP-7 with annealing at 400°C. Indeed, the values of the completely recoverable strain upon bending using these regimes were maximal (8.0 and 9.5%, Fig. 5). The post-deformation annealing at 400°C leads to an increase in the value of the recoverable strain due to a decrease in the transformation yield stress and the retention of the high values of the dislocation yield stress and, as a result, to an increase in their difference $\Delta\sigma$ (Table 2).

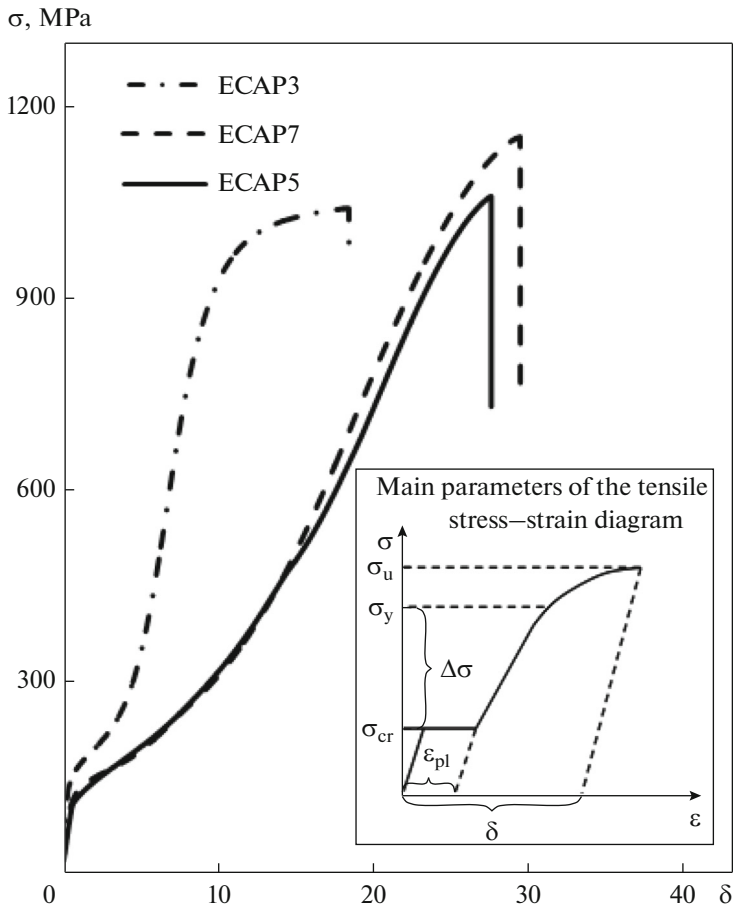

Fig. 4. Tensile stress–strain diagrams for Ti–50.2% Ni alloy after ECAP with different numbers of passes.

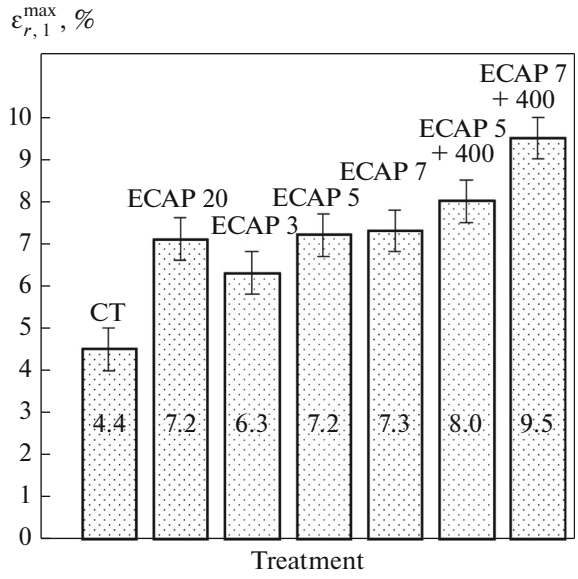

Fig. 5. Maximum completely recoverable strain after CT and different regimes of ECAP.

Table 3. Mechanical properties of the Ti–50.2% Ni alloy

ε_{pl}, %	σ_{cr}, MPa	σ_y, MPa	$\Delta\sigma = \sigma_y - \sigma_{cr}$, MPa	σ_u, MPa	δ, %
HSR					
6.4	100	430	330	700	28
ECAP-3					
5.1	142	855	713	1042	17
ECAP-5					
11.5	157	898	741	1065	22
ECAP-5 + 400°C					
9.7	132	954	822	1060	19
ECAP-7					
10.5	181	941	760	1154	20
ECAP-7 + 400°C					
9.2	125	975	850	1132	21

CONCLUSIONS

(1) Equal channel angular pressing with the intersection angle of channels of 120° at 400°C for seven passes in the quasi-continuous regime was used to produce a mixed nanocrystalline and nanosubgrained structure in the Ti–50.2% Ni alloy with the average size of structural elements of 103 ± 5 nm and high density of free dislocations.

(2) The application of the ECAP method leads to a decrease in the amount of martensite at room temperature, which is associated with a decrease in the M_s point as a result of the deformation work hardening of austenite and an increase in the amount of the *R* phase as a result of the development of chemical inhomogeneity favoring its formation.

(3) The increase in the number of passes from three to seven upon ECAP in the quasi-continuous regime leads to a significant increase in the strength characteristics of the alloy and an insignificant decrease in the plasticity.

(4) The mixed ultrafine-grained structure formed as a result of ECAP increases the realization of the reserve of the recoverable strain; the average value of the maximum completely recoverable strain for Ti–50.2% Ni (at %) alloy after ECAP for five and seven quasi-continuous passes and after periodic ECAP for 20 passes was 7.2–7.3%.

(5) The use of the post-deformation annealing at 400°C leads to an increase in the value of the completely recoverable strain to 8–9.5% due to the decrease in the transformation yield stress with the retention of a high level of dislocation yield stress.

(6) The obtained results confirm the expedience of the use of ECAP as a component of the thermomechanical treatment of Ti–Ni SMAs for production of bulk and long submicro- and nanostructural semifinished materials with high mechanical and functional properties.

ACKNOWLEDGMENTS

This work was supported by the Ministry of Education and Science of the Russian Federation (State task no. 2014/113, project no. 3055, Program of an Increase in the Competitiveness of NUST "MISiS" among the leading world scientific-education centers for 2013–2020, project no. K4-2014-018).

REFERENCES

1. R. Z. Valiev and I. V. Aleksandrov, *Nanostructural Materials Obtained by Severe Plastic Deformation* (Integratsiya, Moscow, 2000).
2. R. Z. Valiev, "Nanomaterial advantage," Nature **419**, 887–889 (2002).
3. I. Yu. Khmelevskaya, S. D. Prokoshkin, S. V. Dobatkin, and V. V. Stolyarov, "Structure and properties of severely deformed Ti–Ni-based shape memory alloys," J. Phys. **4**, 819–822 (2003).
4. I. Yu. Khmelevskaya, I. B. Trubitsyna, S. D. Prokoshkin, S. V. Dobatkin, E. V. Tatyanin, V. V. Stolyarov, and E. A. Prokofiev, "Thermomechanical treatment of Ti–

Ni–based shape memory alloys using severe plastic deformation," Mater. Sci. Forum 426–432, 2765–2770 (2003).

5. S. D. Prokoshkin, I. Yu. Khmelevskaya, S. V. Dobatkin, I. B. Trubitsyna, V. V. Stolyarov, and E. A. Prokofiev, "Structure evolution upon severe plastic deformation of TiNi-based shape–memory alloys," Phys. Met. Metallogr. **97**, 619–625 (2005).
6. S. D. Prokoshkin, I. Y. Khmelevskaya, S. V. Dobatkin, I. B. Trubitsyna, E. V. Tatyanin, V. V. Stolyarov, and E. A. Prokofiev, "Alloy composition, deformation temperature, pressure and post–deformation annealing effects in severely deformed Ti–Ni based shape memory alloys," Act. Mater. **53**, 2703–2714 (2005).
7. I. B. Trubitsina, *Structure Formation and Functional Properties of Ti–Ni Alloys after Severe Plasric Deformation* (NITU MISiS, Moscow, 2005) [in Russian].
8. V. M. Segal, "Plastic treatment of metals by simple shear," Izv. Akad. Nauk SSSR, Met., No. 1, 115–123 (1981).
9. V. M. Segal, "Development of material treatment by severe plastic deformation," Russ. Metall. (Metally) **2004**, 2–9 (2004).
10. R. Z. Valiev and T. G. Langdon, "Principles of equal-channel angular pressing as a processing tool for grain refinement," Progr. Mater. Sci. **51**, 881–981 (2006).
11. G. Raab, "The innovation potential of ECAP techniques of severe plastic deformation," Mater. Sci. Eng. **63**, 012009 (2014).
12. R. Kocich, L. Kunčická, and A. Macháčková, "Twist channel multi-angular pressing (TCMAP) as a new SPD process: Numerical and experimental study," Mater. Sci. Eng., A **612**, 445–455 (2014).
13. A. V. Botkin, "Scientific-Methodological Foundations of Designing Angular-Pressing Processes," *Doctoral (Eng.) Dissertation* (UGATU, Ufa, 2013).
14. D. V. Gunderov, A. V. Polykov, and I. P. Semenova, "Evaluation of microstructure, macrostructure and mechanical properties of commercially pure Ti during ECAP-conform processing and drawing," Mater. Sci. Eng., A **562**, 128–136 (2013).
15. V. V. Stolyarov, E. A. Prokof'ev, S. D. Prokoshkin, S. V. Dobatkin, I. B. Trubitsyna, I. Yu. Khmelevskaya, V. G. Pushin, and R. Z. Valiev,"Structural features, mechanical properties, and the shape-memory effect in TiNi alloys subjected to equal-channel singular pressing," Phys. Met. Metallogr. **100**, 608–612 (2005).
16. V. Brailovski, S. Prokoshkin, I. Khmelevskaya, K. Inaekyan, V. Demers, S. Dobatkin, and E. Tatyanin, "Structure and properties of the Ti–50.0 at % Ni alloy after strain hardening and nanocrystallizing thermomechanical processing," Mater. Trans. **47**, 795–804 (2006).
17. V. Demers, V. Brailovski, S. Prokoshkin, K. Inaekyan, E. Bastarash, I. Khmelevskaya, and S. Dobatkin, "Functional properties of nanostructured Ti–50.0 at % Ni alloy," J. ASTM Int. (JAI) **3**(6), 1–11 (2006).
18. S. D. Prokoshkin, V. Brailovskii, I. Yu. Khmelevskaya, S. V. Dobatkin, K. E. Inaekyan, V. Demers, and E. V. Tat'yanin, "Formation of nanocrystalline structure upon severe rolling plastic deformation and annealing and improvement of set of functional properties of Ti–Ni alloys," Bull. Russ. Acad. Sci.: Phys. **70**, 1536–1541 (2006).
19. V. G. Pushin, R. Z. Valiev, Y. T. Zhu, S. D. Prokoshkin, D. V. Gunderov, and L. I. Yurchenko, "Effect of equal channel angular pressing and repeated rolling on structure phase transformations and properties of TiNi shape memory alloys," Mater. Sci. Forum **503–504**, 539–544 (2006).
20. I. Yu. Khmelevskaya, S. D. Prokoshkin, S. V. Dobatkin, E. V. Tatyanin, and I. B. Trubitsyna, "Studies of composition, deformation temperature and pressure effects on structure formation in severely deformed TiNi–based alloy," Mater. Sci. Eng., A **438–440**, 472–475 (2006).
21. I. Yu. Khmelevskaya, S. D. Prokoshkin, I. B. Trubitsyna, M. N. Belousov, S. V. Dobatkin, E. V. Tatyanin, A. V. Korotitskiy, V. Brailovski, V. V. Stolyarov, and E. A. Prokofiev, "Structure and properties of Ti–Ni-based alloys after equal-channel angular pressing and high-pressure torsion," Mater. Sci. Eng., A **481–482**, 119–122 (2008).
22. D. Gunderov, D. Lukyanov, E. Prokofiev, A. Churakova, V. Pushin, S. Prokoshkin, V. Stolyarov, and R. Valiev, "Microstructure and mechanical properties of the SPD-processed TiNi alloys," Mater. Sci. Forum **738–739**, 486–490 (2013).
23. D. Yu. Zhapova, "Microstructure Evolution and Its Effect on Martensitic Transformations and Nonelastic Properties of Titanium Nickelide-Based Binary Alloys upon Warm Deformation," *Candidate Sci. (Eng.) Dissertation* (IFPM SO RAN, Tomsk, 2013).
24. A. A. Churakova and D. V. Gundarev, "Effect of thermocycling on the temperatures of phase transformations, structure, and properties of the $Ti_{50.0}Ni_{50.0}$ equiatomic alloy," Phys. Met. Metallogr. **117**, 96–106 (2016).
25. H. S. Kim, "Prediction of temperature rise in equal channel angular pressing," Mater. Trans. **42**, 536–538 (2001).
26. H. Shahmir, M. Nili-Ahmadabadi, M. Mansouri-Arani, and T. G. Langdon, "The processing of NiTi shape memory alloys by equal-channel angular pressing at room temperature," Mater. Sci. Eng., A **576**, 178–184 (2013).
27. A. V. Korotitskii, "Express-estimation of parameters of form restoration of shape-memory alloys after deformation induced by bending," in *Proc. 5th Eur.-Asia Sci.Tech. Conf. "Strength of inhomogeneous Structures" PROST 2010* (MISiS, Moscow, 2010).
28. V. Brailovski, S. D. Prokoshkin, P. Terriault, and F. Trochu, *Shape Memory Alloys: Fundamentals, Modeling and Applications* (ETS Publ., Monreal, 2003).
29. S. V. Oleinikova, S. D. Prokoshkin, L. M. Kaputkina, I. Yu. Khmelevskaya, A. A. Kadnikov, and L. A. Zaitseva, "Effect of ageing on mechanical behavior of Ti–50.7% Ni alloy," Tekhnol. Legk. Splavov, No. **4**, 28–34 (1990).

30. V. Brailovski, S. Prokoshkin, K. Inaekyan, and V. Demers, "Functional properties of nanocrystalline, submicrocrystalline and polygonized Ti–Ni alloys processed by cold rolling and post-deformation annealing," J. Alloys Compd. **509**, 2066–2075 (2011).

31. K. A. Polyakova-Vachiyan, E. P. Ryklina, S. D. Prokoshkin, and S. M. Dubinskii, "Dependence of the functional characteristics of thermomechanically processed titanium nickelide on the size of the structural elements of austenite," Phys. Met. Metallogr. **117**, 817–827 (2016).

32. S. D. Prokoshkin, V. Brailovskii, A. V. Korotitskii, K. E. Inaekyan, and A. M. Glezer, "Specific features of the formation of the microstructure of titanium nickelide upon thermomechanical treatment including cold plastic deformation to degrees from moderate to severe," Phys. Met. Metallogr. **110**, 289–303 (2010).

33. S. D. Prokoshkin, I. Yu. Khmelevskaya, V. Brailovski, F. Trochu, and V. Y. Turilina, "Structure and deformation diagrams of NiTi alloys subjected to a low-temperature thermomechanical treatment with postdeformation heating," Phys. Met. Metallogr. **91**, 423–431 (2001).

34. A. Kreitcberg, V. Brailovski, S. Prokoshkin, D. Gunderov, M. Khomutov, and K. Inaekyan, "Effect of the grain/subgrain size on the strain-rate sensitivity and deformability of Ti–50 at %Ni alloy," Mater. Sci. Eng., A **622**, 21–29 (2015).

Translated by O. Golosova